

Diffuse optical monitoring of repeated cerebral ischemia in mice

Yu Shang,¹ Lei Chen,² Michal Toborek,² and Guoqiang Yu^{1,*}

¹Center for Biomedical Engineering, University of Kentucky, Lexington, Kentucky 40506, USA

²Department of Neurosurgery, University of Kentucky, Lexington, Kentucky 40536, USA

*guoqiang.yu@uky.edu

Abstract: Occlusions of bilateral common carotid arteries (bi-CCA) in mice are popular models for the investigation of transient forebrain ischemia. Currently available technologies for assessing cerebral blood flow (CBF) and oxygenation in ischemic mice have limitations. This study tests a novel near-infrared diffuse correlation spectroscopy (DCS) flow-oximeter for monitoring both CBF and cerebral oxygenation in mice undergoing repeated transient forebrain ischemia. Concurrent flow measurements in a mouse brain were first conducted for validation purposes; DCS measurement was found highly correlated with laser Doppler measurement ($R^2 = 0.94$) and less susceptible to motion artifacts. With unique designs in experimental protocols and fiber-optic probes, we have demonstrated high sensitivities of DCS flow-oximeter in detecting the regional heterogeneity of CBF responses in different hemispheres and global changes of both CBF and cerebral oxygenation across two hemispheres in mice undergoing repeated 2-minute bi-CCA occlusions over 5 days. More than 75% CBF reductions were found during bi-CCA occlusions in mice, which may be considered as a threshold to determine a successful bi-CCA occlusion. With the progress of repeated 2-minute bi-CCA occlusions over days, a longitudinal decline in the magnitudes of CBF reduction was observed, indicating the brain adaptation to cerebral ischemia through the repeated preconditioning.

©2011 Optical Society of America

OCIS codes: (170.0170) Medical optics and biotechnology; (170.3660) Light propagation in tissues; (170.3880) Medical and biological imaging; (170.6480) Spectroscopy, speckle.

References and links

1. G. Pignataro, A. Scorziello, G. Di Renzo, and L. Annunziato, "Post-ischemic brain damage: effect of ischemic preconditioning and postconditioning and identification of potential candidates for stroke therapy," *FEBS J.* **276**(1), 46–57 (2009).
2. T. Kirino, "Ischemic tolerance," *J. Cereb. Blood Flow Metab.* **22**(11), 1283–1296 (2002).
3. A. Durukan, D. Strbian, and T. Tatlisumak, "Rodent models of ischemic stroke: a useful tool for stroke drug development," *Curr. Pharm. Des.* **14**(4), 359–370 (2008).
4. B. Schaller and R. Graf, "Cerebral ischemic preconditioning," *J. Neurol.* **249**(11), 1503–1511 (2002).
5. N. E. Stagliano, M. A. Pérez-Pinzón, M. A. Moskowitz, and P. L. Huang, "Focal ischemic preconditioning induces rapid tolerance to middle cerebral artery occlusion in mice," *J. Cereb. Blood Flow Metab.* **19**(7), 757–761 (1999).
6. J. M. Gidday, "Cerebral preconditioning and ischaemic tolerance," *Nat. Rev. Neurosci.* **7**(6), 437–448 (2006).
7. R. R. Ratan, A. Siddiq, L. Aminova, P. S. Lange, B. Langley, I. Ayoub, J. A. Gensert, and J. Chavez, "Translation of ischemic preconditioning to the patient - Prolyl hydroxylase inhibition and hypoxia inducible factor-1 as novel targets for stroke therapy," *Stroke* **35**(11,Suppl. 1), 2687–2689 (2004).
8. K. Kitagawa, M. Matsumoto, G. M. Yang, T. Mabuchi, Y. Yagita, M. Hori, and T. Yanagihara, "Cerebral ischemia after bilateral carotid artery occlusion and intraluminal suture occlusion in mice: Evaluation of the patency of the posterior communicating artery," *J. Cereb. Blood Flow Metab.* **18**(5), 570–579 (1998).
9. L. Chen, K. R. Swartz, and M. Toborek, "Vessel microport technique for applications in cerebrovascular research," *J. Neurosci. Res.* **87**(7), 1718–1727 (2009).
10. R. S. Marshall, T. Rundek, D. M. Sproule, B. F. M. Fitzsimmons, S. Schwartz, and R. M. Lazar, "Monitoring of cerebral vasodilatory capacity with transcranial Doppler carbon dioxide inhalation in patients with severe carotid artery disease," *Stroke* **34**(4), 945–949 (2003).

11. Y. Shang, R. Cheng, L. Dong, S. J. Ryan, S. P. Saha, and G. Yu, "Cerebral monitoring during carotid endarterectomy using near-infrared diffuse optical spectroscopies and electroencephalogram," *Phys. Med. Biol.* **56**(10), 3015–3032 (2011).
12. P. J. Goadsby and L. Edvinsson, *Neurovascular control of the cerebral circulation*, (Lippincott Williams & Wilkins, 2002).
13. N. Khan, B. B. Williams, H. Hou, H. Li, and H. M. Swartz, "Repetitive tissue pO₂ measurements by electron paramagnetic resonance oximetry: current status and future potential for experimental and clinical studies," *Antioxid. Redox Signal.* **9**(8), 1169–1182 (2007).
14. H. Piilgaard and M. Lauritzen, "Persistent increase in oxygen consumption and impaired neurovascular coupling after spreading depression in rat neocortex," *J. Cereb. Blood Flow Metab.* **29**(9), 1517–1527 (2009).
15. P. Riyamongkol, W. Z. Zhao, Y. T. Liu, L. Belayev, R. Busto, and M. D. Ginsberg, "Automated registration of laser Doppler perfusion images by an adaptive correlation approach: application to focal cerebral ischemia in the rat," *J. Neurosci. Methods* **122**(1), 79–90 (2002).
16. A. B. Parthasarathy, S. M. Kazmi, and A. K. Dunn, "Quantitative imaging of ischemic stroke through thinned skull in mice with Multi Exposure Speckle Imaging," *Biomed. Opt. Express* **1**(1), 246–259 (2010).
17. J. Luckl, W. Baker, Z. H. Sun, T. Durduran, A. G. Yodh, and J. H. Greenberg, "The biological effect of contralateral forepaw stimulation in rat focal cerebral ischemia: a multispectral optical imaging study," *Front. Neuroenergetics* **2** (2010).
18. L. F. Yu, E. Nguyen, G. J. Liu, B. Choi, and Z. P. Chen, "Spectral Doppler optical coherence tomography imaging of localized ischemic stroke in a mouse model," *J. Biomed. Opt.* **15**(6), 066006 (2010).
19. Y. L. Jia and R. K. K. Wang, "Optical micro-angiography images structural and functional cerebral blood perfusion in mice with cranium left intact," *J. Biophoton.* **4**(1-2), 57–63 (2011).
20. A. Van der Linden, N. Van Camp, P. Ramos-Cabrer, and M. Hoehn, "Current status of functional MRI on small animals: application to physiology, pathophysiology, and cognition," *NMR Biomed.* **20**(5), 522–545 (2007).
21. Y. Kuge, H. Kawashima, T. Hashimoto, M. Imanishi, M. Shiomi, K. Minematsu, Y. Hasegawa, T. Yamaguchi, Y. Miyake, and N. Hashimoto, "Preliminary evaluation of [1-¹¹C]octanoate as a PET tracer for studying cerebral ischemia: a PET study in rat and canine models of focal cerebral ischemia," *Ann. Nucl. Med.* **14**(1), 69–74 (2000).
22. S. Fantini, D. Hueber, M. A. Franceschini, E. Gratton, W. Rosenfeld, P. G. Stubblefield, D. Maulik, and M. R. Stankovic, "Non-invasive optical monitoring of the newborn piglet brain using continuous-wave and frequency-domain spectroscopy," *Phys. Med. Biol.* **44**(6), 1543–1563 (1999).
23. F. H. Tian, B. Chance, and H. L. Liu, "Investigation of the prefrontal cortex in response to duration-variable anagram tasks using functional near-infrared spectroscopy," *J. Biomed. Opt.* **14**(5), 054016 (2009).
24. M. A. Franceschini, D. K. Joseph, T. J. Huppert, S. G. Diamond, and D. A. Boas, "Diffuse optical imaging of the whole head," *J. Biomed. Opt.* **11**(5), 054007 (2006).
25. G. Strangman, M. A. Franceschini, and D. A. Boas, "Factors affecting the accuracy of near-infrared spectroscopy concentration calculations for focal changes in oxygenation parameters," *Neuroimage* **18**(4), 865–879 (2003).
26. T. Durduran, "Non-Invasive Measurements of Tissue Hemodynamics with Hybrid Diffuse Optical Methods," Degree of Doctor of Philosophy (University of Pennsylvania, 2004).
27. X. Intes, C. Maloux, M. Guven, B. Yazici, and B. Chance, "Diffuse optical tomography with physiological and spatial a priori constraints," *Phys. Med. Biol.* **49**(12), N155–N163 (2004).
28. J. P. Culver, T. Durduran, D. Furuya, C. Cheung, J. H. Greenberg, and A. G. Yodh, "Diffuse optical tomography of cerebral blood flow, oxygenation, and metabolism in rat during focal ischemia," *J. Cereb. Blood Flow Metab.* **23**(8), 911–924 (2003).
29. J. Li, M. Ninck, L. Koban, T. Elbert, J. Kissler, and T. Gislser, "Transient functional blood flow change in the human brain measured noninvasively by diffusing-wave spectroscopy," *Opt. Lett.* **33**(19), 2233–2235 (2008).
30. L. Gagnon, M. Desjardins, J. Jehanne-Lacasse, L. Bherer, and F. Lesage, "Investigation of diffuse correlation spectroscopy in multi-layered media including the human head," *Opt. Express* **16**(20), 15514–15530 (2008).
31. T. Durduran, G. Yu, M. G. Burnett, J. A. Detre, J. H. Greenberg, J. J. Wang, C. Zhou, and A. G. Yodh, "Diffuse optical measurement of blood flow, blood oxygenation, and metabolism in a human brain during sensorimotor cortex activation," *Opt. Lett.* **29**(15), 1766–1768 (2004).
32. G. Yu, T. F. Floyd, T. Durduran, C. Zhou, J. J. Wang, J. A. Detre, and A. G. Yodh, "Validation of diffuse correlation spectroscopy for muscle blood flow with concurrent arterial spin labeled perfusion MRI," *Opt. Express* **15**(3), 1064–1075 (2007).
33. D. A. Boas, L. E. Campbell, and A. G. Yodh, "Scattering and Imaging with Diffusing Temporal Field Correlations," *Phys. Rev. Lett.* **75**(9), 1855–1858 (1995).
34. G. Yu, T. Durduran, C. Zhou, H. W. Wang, M. E. Putt, H. M. Saunders, C. M. Sehgal, E. Glatstein, A. G. Yodh, and T. M. Busch, "Noninvasive monitoring of murine tumor blood flow during and after photodynamic therapy provides early assessment of therapeutic efficacy," *Clin. Cancer Res.* **11**(9), 3543–3552 (2005).
35. R. C. Mesquita, N. Skuli, M. N. Kim, J. Liang, S. Schenkel, A. J. Majmundar, M. C. Simon, and A. G. Yodh, "Hemodynamic and metabolic diffuse optical monitoring in a mouse model of hindlimb ischemia," *Biomed. Opt. Express* **1**(4), 1173–1187 (2010).
36. M. N. Kim, T. Durduran, S. Frangos, B. L. Edlow, E. M. Buckley, H. E. Moss, C. Zhou, G. Yu, R. Choe, E. Maloney-Wilensky, R. L. Wolf, M. S. Grady, J. H. Greenberg, J. M. Levine, A. G. Yodh, J. A. Detre, and W. A. Kofke, "Noninvasive Measurement of Cerebral Blood Flow and Blood Oxygenation Using Near-Infrared and Diffuse Correlation Spectroscopies in Critically Brain-Injured Adults," *Neurocrit. Care* **12**(2), 173–180 (2010).

37. E. M. Buckley, N. M. Cook, T. Durduran, M. N. Kim, C. Zhou, R. Choe, G. Yu, S. Schultz, C. M. Sehgal, D. J. Licht, P. H. Arger, M. E. Putt, H. H. Hurt, and A. G. Yodh, "Cerebral hemodynamics in preterm infants during positional intervention measured with diffuse correlation spectroscopy and transcranial Doppler ultrasound," *Opt. Express* **17**(15), 12571–12581 (2009).
38. C. Zhou, S. A. Eucker, T. Durduran, G. Yu, J. Ralston, S. H. Friess, R. N. Ichord, S. S. Margulies, and A. G. Yodh, "Diffuse optical monitoring of hemodynamic changes in piglet brain with closed head injury," *J. Biomed. Opt.* **14**(3), 034015 (2009).
39. U. Sunar, H. Quon, T. Durduran, J. Zhang, J. Du, C. Zhou, G. Yu, R. Choe, A. Kilger, R. Lustig, L. Loevner, S. Nioka, B. Chance, and A. G. Yodh, "Noninvasive diffuse optical measurement of blood flow and blood oxygenation for monitoring radiation therapy in patients with head and neck tumors: a pilot study," *J. Biomed. Opt.* **11**(6), 064021 (2006).
40. Y. Shang, Y. Zhao, R. Cheng, L. Dong, D. Irwin, and G. Yu, "Portable optical tissue flow oximeter based on diffuse correlation spectroscopy," *Opt. Lett.* **34**(22), 3556–3558 (2009).
41. G. Yu, Y. Shang, Y. Zhao, R. Cheng, L. Dong, and S. P. Saha, "Intraoperative evaluation of revascularization effect on ischemic muscle hemodynamics using near-infrared diffuse optical spectroscopies," *J. Biomed. Opt.* **16**(2), 027004 (2011).
42. C. Cheung, J. P. Culver, K. Takahashi, J. H. Greenberg, and A. G. Yodh, "In vivo cerebrovascular measurement combining diffuse near-infrared absorption and correlation spectroscopies," *Phys. Med. Biol.* **46**(8), 2053–2065 (2001).
43. A. Duncan, J. H. Meek, M. Clemence, C. E. Elwell, L. Tyszczyk, M. Cope, and D. T. Delpy, "Optical pathlength measurements on adult head, calf and forearm and the head of the newborn infant using phase resolved optical spectroscopy," *Phys. Med. Biol.* **40**(2), 295–304 (1995).
44. Y. Shang, T. B. Symons, T. Durduran, A. G. Yodh, and G. Yu, "Effects of muscle fiber motion on diffuse correlation spectroscopy blood flow measurements during exercise," *Biomed. Opt. Express* **1**(2), 500–511 (2010).
45. B. Chance, M. T. Dait, C. D. Zhang, T. Hamaoka, and F. Hagerman, "Recovery from Exercise-Induced Desaturation in the Quadriceps Muscles of Elite Competitive Rowers," *Am. J. Physiol.* **262**(3 Pt 1), C766–C775 (1992).
46. H. W. Wang, M. E. Putt, M. J. Emanuele, D. B. Shin, E. Glatstein, A. G. Yodh, and T. M. Busch, "Treatment-induced changes in tumor oxygenation predict photodynamic therapy outcome," *Cancer Res.* **64**(20), 7553–7561 (2004).
47. M. J. Leahy, F. F. de Mul, G. E. Nilsson, and R. Maniewski, "Principles and practice of the laser-Doppler perfusion technique," *Technol. Health Care* **7**(2-3), 143–162 (1999).
48. K. Kidoguchi, M. Tamaki, T. Mizobe, J. Koyama, T. Kondoh, E. Kohmura, T. Sakurai, K. Yokono, and K. Umetani, "In vivo X-ray angiography in the mouse brain using synchrotron radiation," *Stroke* **37**(7), 1856–1861 (2006).
49. D. Irwin, L. Dong, Y. Shang, R. Cheng, M. Kudrimoti, S. D. Stevens, and G. Yu, "Influences of tissue absorption and scattering on diffuse correlation spectroscopy blood flow measurements," *Biomed. Opt. Express* **2**(7), 1969–1985 (2011).
50. J. Hendrikse, M. J. Hartkamp, B. Hillen, W. P. T. M. Mali, and J. van der Grond, "Collateral ability of the circle of Willis in patients with unilateral internal carotid artery occlusion: Border zone infarcts and clinical symptoms," *Stroke* **32**(12), 2768–2773 (2001).
51. L. F. Liu, C. K. Yeh, C. H. Chen, T. W. Wong, and J. J. J. Chen, "Measurement of Cerebral Blood Flow and Oxygen Saturation Using Laser Doppler Flowmetry and Near Infrared Spectroscopy in Ischemic Stroke Rats," *Med. Biol. Eng.* **28**, 101–105 (2008).
52. P. T. Ulrich, S. Kroppenstedt, A. Heimann, O. Kempfski, and B. G. Lyeth, "Laser-Doppler scanning of local cerebral blood flow and reserve capacity and testing of motor and memory functions in a chronic 2-vessel occlusion model in rats," *Stroke* **29**(11), 2412–2420 (1998).

1. Introduction

Stroke is the third cause of death in US with over 700,000 occurrences, 200,000 deaths and more disabilities annually [1]. Cerebral ischemic stroke accounts for approximately 80% stroke cases [2]. Animal models of cerebral ischemia contribute greatly to the understanding of stroke pathophysiology [3]. Mouse is the often used animal for stroke studies because of the low cost and wide spectrum of transgenic strains [3–5]. The duration and frequency of cerebral ischemia and the interval between occurrences can significantly affect neuronal viability and vascular response, resulting in different pathophysiological consequences [1, 2, 6]. The short-term less-injurious interruptions (e.g., 2 minutes) of cerebral blood flow (CBF) enable the neurons to obtain the protection against the subsequently long episode of ischemia and enhance the cerebral ischemic tolerance, which is known as cerebral ischemic preconditioning [1, 2, 4, 6, 7]. Preconditioning may also reduce the thereafter ischemia-reperfusion (I-R) injury [1]. By contrast, the medium-term cerebral ischemia (e.g., 10 minutes) could induce transient ischemic

attack (TIA) [2], the prognostic of stroke. Either preconditioning or TIA requires multi-day repeated transient ischemia for the accumulation of cerebral protection or injury [2,4]. The transient forebrain ischemia of preconditioning or TIA in mice is usually induced by temporary occlusion of bilateral common carotid arteries (bi-CCA) [4,8].

A successful bi-CCA occlusion is critical for setting up a reliable forebrain ischemic model. Real-time monitoring of CBF reductions provides an objective way to assess the success of CCA occlusion [4, 8, 9]. Noninvasive or minimally-invasive CBF measurements are particularly important for the repeated cerebral ischemia studies which require animals to survive over several days [2, 4]. Moreover, quantification of CBF responses to I-R challenges allows for the assessment of cerebral vasodilatations [10, 11], which are involved in neuron protection/injury mechanism of preconditioning/TIA [6, 12]. Measurements of cerebral oxygenation in ischemic mice are also critical since cerebral oxygenation level reflects cerebrovascular reactivity, neuronal viability and cerebral metabolism [7, 13].

Techniques currently available for monitoring of cerebral hemodynamics in mice have limitations. Partial pressure of oxygen (PO_2) electrode is an invasive tool for measurement of cerebral oxygenation at a single tiny spot [13]. Although laser Doppler flowmetry (LDF) is the most frequently used tool in mouse studies, it detects blood flow at a single tiny spot of the superficial cortex (~1 mm depth) [14], which may not reflect the CBF in deep brain. Moreover, laser Doppler measurement requires aligning a small fiber-optic probe on top of a small vessel branch, thus introducing the difficulty for probe installation and increasing the sensitivity to motion artifacts. Similar to LDF, laser Doppler imaging (LDI) [15], laser speckle imaging (LSI) [16, 17], Doppler optical coherence tomography (DOCT) [18], optical micro-angiography (OMAG) [19] and optical imaging of intrinsic signals (OIS) can be used for mapping CBF or oxygenation at only superficial cortex of ischemic mouse and rat brains. Although functional Magnetic Resonance Imaging (fMRI) or Positron Emission Tomography (PET) can generate hemodynamic images of mouse brain [20, 21], the high cost and low mobility preclude their wide uses in experimental animals.

Near-infrared diffuse optical spectroscopy (NIRS) offers a noninvasive, rapid, portable, and low-cost alternative for the monitoring of cerebral blood oxygenation in deep microvasculature [22–27]. A well known spectral window exists in near-infrared (NIR) range (650-950 nm) wherein tissue absorption is relatively low so that light can penetrate into deep/thick volumes of tissue (up to centimeters). The difference of major tissue chromophores in NIR absorption spectra allows for the measurement of oxygenated and deoxygenated hemoglobin concentrations. NIR diffuse correlation spectroscopy (DCS) is an emerging technique capable of noninvasive CBF measurement [11, 28–31]. DCS measures light intensity fluctuations from a single speckle area of tissue surface, which are directly correlated with the motion of red blood cells in microvasculature of deep tissues [26, 32, 33]. Measurements of blood flow variations by DCS in various organs/tissues have been compared and validated to other standards, including power Doppler ultrasound [34], LDF [26, 35], Xenon-CT [36], Doppler ultrasound [37], fluorescent microsphere measurement of CBF [38], perfusion MRI [31, 32], and histology and nitroimidazole hypoxia markers (EF5) [39]. Based on the DCS technique, we recently developed and validated a portable and easy-to-use diffuse optical instrument (namely DCS flow-oximeter) for simultaneous measurements of blood flow and oxygenation in deep tissues [40]. This new instrument has been recently used in clinic to monitor variations of tissue hemodynamics in ischemic muscle/brain during femoral arterial revascularization/carotid endarterectomy surgery [11, 41].

DCS technologies were also used for cerebral monitoring in some animals including piglet [38] and rat [26, 28]. However, they have not been applied to mouse brains. One challenge for the use of NIRS/DCS technologies in mouse brain is the small size of mouse head, making the installation of fiber-optic probes difficult. Another challenge is to design probes that can be repeatedly used for longitudinal monitoring of multi-day transient ischemia. In this report, we demonstrate the *first* continuous and longitudinal monitoring of both CBF and cerebral

oxygenation in transient ischemic mice using the novel DCS flow-oximeter and custom-designed fiber-optic probes. A series of experiments were designed to comprehensively evaluate the capability and sensitivity of DCS flow-oximeter in detecting regional and global CBF/oxygenation in mice undergoing repeated transient forebrain ischemia. Cerebral hemodynamic changes during repeated forebrain ischemia were quantified and used for guiding proper arterial occlusions and evaluating preconditioning effects on cerebral ischemia/hypoxia adaptation. Concurrent CBF measurements in a mouse brain by DCS and commercial LDF were also conducted for validation purposes.

2. Materials and methods

2.1 NIR DCS flow-oximeter

DCS flow-oximeter for tissue blood flow measurement. A custom-designed dual-wavelength DCS flow-oximeter (see Fig. 1a) was recently developed for simultaneous measurements of CBF and cerebral oxygenation in deep tissues [40]. Briefly, it consists of two laser diodes (785 and 854 nm, Crystalaser Inc., NV, USA) with long coherence length (> 5 meters), four single-photon-counting avalanche photodiode (APD) detectors (PerkinElmer Inc., Canada), and a four-channel correlator (correlator.com, NJ, USA) (see Fig. 1b). Photons are emitted from the laser sources through multi-mode source fibers (diameter = 200 μm), travel through the tissue, and are scattered back to the detectors through single-mode detector fibers (diameter = 5.6 μm). The correlator takes the detector outputs and uses photon arrival times to compute the light intensity autocorrelation function. From the normalized intensity autocorrelation function, we calculate the electric field temporal autocorrelation function $G_I(\mathbf{r}, \tau)$, which satisfies the correlation diffusion equation in highly scattering media [33]. Here \mathbf{r} is the source-detector (S-D) separation and τ is the delay time. For semi-infinite homogeneous tissue, $G_I(\mathbf{r}, \tau)$ is a function of tissue absorption coefficient μ_a and reduced scattering coefficient μ_s , as well as the mean-square displacement $\langle \Delta \mathbf{r}^2(\tau) \rangle$ of moving scatterers in tissue (primarily red blood cells) [26, 42]. For the case of diffusive motion, $\langle \Delta \mathbf{r}^2(\tau) \rangle = 6D_B\tau$, where D_B is an *effective* diffusion coefficient of the moving scatterers. In this case the autocorrelation function $G_I(\mathbf{r}, \tau)$ decays approximately exponentially in the decay time τ . Its decay rate, Γ (sec^{-1}), depends on a parameter α (proportional to the tissue red blood cell volume fraction), and on the motion of red blood cells. The blood flow index (αD_B) is then derived by fitting the measured autocorrelation curve to the analytical solution of $G_I(\mathbf{r}, \tau)$ [26, 32, 42]. Similar to many other studies using DCS for tissue blood flow measurements [11, 37, 41], we used the constant values of μ_a and μ_s determined based on the literatures [26,28] to calculate the blood flow index.

DCS flow-oximeter for tissue blood oxygenation measurement. DCS for blood flow measurement needs only one wavelength of light source. Adding a second NIR laser to DCS device allows for simultaneous measurements of tissue blood oxygenation [40]. As shown in Fig. 1b, two laser diodes (785 and 854 nm) are turned on alternatively by a transistor-transistor logic (TTL) control unit, launching the photons into the tissue sequentially. Some of the emitted photons are absorbed by tissue absorbers (mainly hemoglobin) when they travel through the tissue from the source to the detector, leading to an intensity reduction in detected light. The relative change in tissue absorption coefficient ($\Delta\mu_a$) can be derived from the change of detected light intensity. Changes of oxygenated and deoxygenated hemoglobin concentrations ($\Delta[\text{HbO}_2]$ and $\Delta[\text{Hb}]$) relative to their baseline values (determined before physiological changes) can be calculated from the measured $\Delta\mu_a$ at two wavelengths, using the modified Beer-Lambert Law [25]. According to the Modified Beer-Lambert Law, mean photon pathlength depends on the S-D separation and a wavelength-dependent differential pathlength factor (DPF). In the present study, the S-D separations were set up in a range of 5.0 to 7.5 mm for different experiments (see Section 2.3) and the DPFs at different wavelengths were determined based on the literature [43]. Use of the two wavelengths (785 and 854 nm) for tissue

blood oxygenation measurement has been previously validated against a commercial tissue oximeter (Imagent, ISS Inc., IL, USA) [40]. Optimization of wavelengths [25] to obtain maximum detection sensitivity will be the subject of future work.

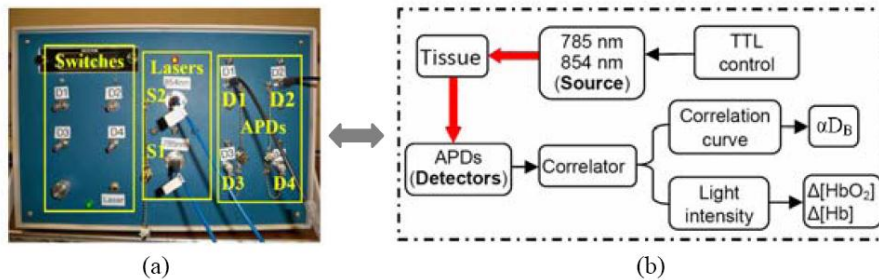


Fig. 1. (a) Photography of DCS flow-oximeter. (b) Diagram of DCS flow-oximeter.

Probing depth and sampling rate. DCS flow-oximeter has been used in various human tissues with diverse probes [11, 40, 41, 44]. In the present study, several fiber-optic probes with source-detector (S-D) separations of 5.0 to 7.5 mm are designed for use on mouse heads undergoing different experimental protocols (see Section 2.3). Based on the photon diffusion theory, the maximum penetration depth of NIR light in tissue depends on tissue optical properties and the S-D separation, and is roughly one-half of the S-D separation [45]. DCS flow-oximeter thus probes a depth of 2.5 to 3.5 mm beneath the skull. Notice that although the use of diffusion approximation of light transport in small mouse brain as well as assumed optical properties (i.e., DPF, μ_a and μ_s) may affect the evaluation accuracies of CBF and oxygenation, the approximation/assumption has been previously used in NIRS/DCS data analysis for other small species/organs such as rat brain [26, 28, 42], mouse tumor [34, 46] and mouse leg muscle [35]. The S-D separations used in those studies varied from 1.0 to 10.0 mm, which cover the range of the S-D separations (5.0 to 7.5 mm) used in the present study. Particularly in some of those studies, flow/oxygenation measurements were validated by comparing to other standards such as color-weighted Doppler ultrasound [34], laser Doppler [35] and O_2 electrode [46].

The sampling time of DCS flow-oximeter is 2.4 seconds (0.4 Hz) for a complete frame of blood flow and oxygenation measurements (1.2 seconds for each wavelength), which is short enough for recording the relatively long periods (≥ 2 minutes) of ischemic events.

2.2 Mouse model of repeated transient forebrain ischemia

A unique mouse model with repeated transient forebrain ischemia is created in the present study. The C57BL/6 mouse (male, 10 to 12 weeks old, Harlan Laboratories Inc., IN, USA) is anesthetized by the inhalation of 1 to 2% isoflurane in oxygen throughout ischemic procedure and its rectal temperature is maintained at 37°C with a warm blanket [9]. The scalp of anesthetized mouse is surgically removed to expose the skull for the installation of optical probes. The basilar artery and right internal carotid artery (RCCA) are isolated and permanently ligated. A customized vascular occluder with its actuating tubing glued to a microport is cuffed around the isolated left internal carotid artery (LCCA) and secured with surgical sutures. Through the subcutaneously buried microport, air is injected or withdrawn with a syringe to inflate or deflate the occluder diaphragm, thus occluding the LCCA (forebrain ischemia) or allowing for the restoration of blood flow (reperfusion), respectively. After the surgical wound is closed, the mouse is returned to cage for recovery. Thereafter, the mouse is subjected to repeated forebrain ischemia by air injection through the microport to pressurize the occluder diaphragm for 2 minutes/time/day up to 5 I-R cycles. This model can repeat forebrain I-R challenges without heart arrest or multiple surgeries; it mimics repeated preconditioning against TIA and stroke.

2.3 Experimental protocols

To evaluate the use of DCS flow-oximeter for cerebral monitoring in mice, three experimental protocols were designed, including a comparison of CBF measurements by DCS and LDF, regional and global CBF measurements in two hemispheres, and simultaneous measurements of CBF and cerebral blood oxygenation in mice undergoing repeated transient ischemia. These experimental protocols were approved by the Institutional Animal Care and Use Committee in accordance with the National Institutes of Health guidelines.

Protocol #1: Comparison of CBF measurements by DCS and LDF during CCA occlusion. Although DCS has been broadly validated against other established techniques, including LDF in mouse muscle [35] and rat brain [26], the validation has not been done in mouse brain. The comparison of DCS and LDF (PeriFlux System 5000, Perimed Inc.) for CBF measurements in a mouse was explored in this experiment. As shown in Fig. 2a, a small LDF probe (integrating one pair of source and detector fibers) and a DCS detector fiber were confined in a foam pad which was glued on the mouse skull. The LDF probe was aligned to a small branch of middle cerebral artery (MCA) and measured CBF at the superficial cortex (~1 mm beneath the skull). DCS shared the long coherence LDF source at 780 nm. The separation between the source (S) and detector (D) fibers for DCS was 5.0 mm, allowing for probing a depth up to ~2.5 mm. The mouse underwent unilateral CCA clipping once and bi-CCA clipping/unclipping twice to induce CBF changes, and mouse CBF was concurrently measured by the DCS and LDF.

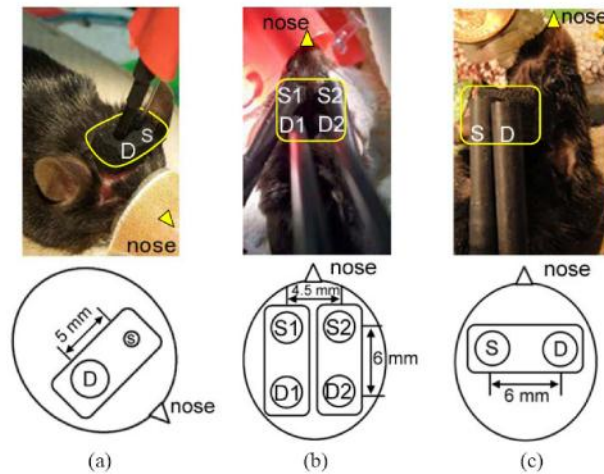


Fig. 2. (a) Installation of a LDF probe and DCS detector fiber on mouse skull. S: LDF probe (integrating one pair of source and detector fibers); D: DCS detector fiber. (b) Installation of two DCS probes on two sides of mouse head. S1 and S2: DCS source fibers; D1 and D2: DCS detector fibers. (c) Installation of a single DCS probe on mouse skull. S: two DCS source fibers (tightly bundled and placed at the same location); D: DCS detector fiber.

Protocol #2: Regional and global CBF measurements during CCA occlusion. This protocol is designed to exam the use of DCS flow-oximeter for detecting both regional (in each of two hemispheres) and global (across hemispheres) CBF changes. Ten mice were tested in this protocol and the CCA clipping/unclipping was used to induce CBF changes. As shown in Fig. 2b, two pairs (S1-D1, S2-D2) of source (S) and detector (D) fibers confined in two foam pads were glued on the two sides of mouse skull respectively, allowing for simultaneous measurements of CBF in left and right hemispheres. The optical fibers were connected to a dual-wavelength DCS flow-oximeter which turned on and off the two laser sources (S1 and S2) alternatively and measured CBF in each hemisphere sequentially. The two detectors (D1 and D2) collected the optical signals in parallel. The left (S1-D1) and right (S2-D2) fiber pairs with

a S-D separation of 6.0 mm measured the regional CBF changes in left and right hemispheres, respectively. Other S-D pairs (S1-D2 and S2-D1) with a S-D separation of 7.5 ($\sqrt{4.5^2 + 6^2}$) mm covered the brain tissues across the two hemispheres, thus reflecting the “global” (i.e., across-regional) CBF changes. The S-D separations of 6.0 to 7.5 mm allowed for probing a depth up to ~3.5 mm. The regional and global CBF changes were continuously monitored during CCA clipping/unclipping.

Protocol #3: Simultaneous measurements of CBF and cerebral blood oxygenation during repeated transient forebrain ischemia. This protocol is designed to exam the use of DCS flow-oximeter for simultaneously assessing CBF and cerebral blood oxygenation in mice undergoing repeated transient forebrain ischemia. Ten mice undergoing multiple 2-minute bi-CCA occlusions over 5 days were tested. As shown in Fig. 2c, two DCS source fibers were tightly bundled and placed at the same location (S) and connected to the two DCS lasers (785 and 854 nm). The source fiber bundle (S) and one detector fiber (D) were confined with a separation of 6.0 mm by a foam pad that was glued on the skull across the two hemispheres. The source and detector fibers were connected to a dual-wavelength DCS flow-oximeter, allowing for simultaneous measurements of global CBF and cerebral blood oxygenation across the two hemispheres at a depth of ~3 mm beneath the skull. At Day 1, the mouse underwent a unilateral CCA ligation, followed by a 2-minute bi-CCA occlusion. Thereafter, the mouse received the 2-minute I-R challenge (bi-CCA occlusion) once per day over 5 days/cycles. Mouse CBF and cerebral blood oxygenation were continuously monitored during each period of I-R challenge. Note that the foam pad used to confine the source and detector fibers was permanently glued on the mouse skull before initiating the surgery and it stayed on the skull over 5 days. However, the optical fibers were removed off the pad each day after the optical measurement and inserted back into the pad before the next optical measurement in the following day. This special design allowed for longitudinal monitoring of CBF/oxygenation at the same location of mouse brain, and avoided the interruption of optical fibers on mouse daily activities.

2.4 Data analysis

Following the methods used in previous studies for the quantification of tissue hemodynamic changes [11, 31, 32, 40, 41, 44], the percentage changes of CBF are calculated for the evaluation of cerebral ischemia during CCA occlusions. The CBF (i.e., αD_B) is normalized to its baseline (assigned to be 100%), i.e., mean value of the 1-minute CBF data (~25 data points) right before the arterial occlusion. Similarly, the changes of oxygenated and deoxygenated hemoglobin concentrations ($\Delta[\text{HbO}_2]$ and $\Delta[\text{Hb}]$) relative to their 1-minute baseline values (assigned to be 0) are calculated respectively for the evaluation of cerebral hypoxia induced by cerebral ischemia. The relative changes in CBF and oxygenation over the durations of unilateral and 2-minute bilateral CCA occlusions are averaged respectively for the quantification of cerebral hemodynamic responses to cerebral arterial occlusions. The average hemodynamic responses over mice are presented as means \pm standard errors (error bars) in figures. Linear regression is used to exam the correlation of CBF measurements by two different methods (i.e., DCS and LDF). Student *t*-test is used to test the significances in hemodynamic changes. The criterion for significance is $p < 0.05$.

3. Results

3.1 Protocol #1: comparison of CBF measurements by DCS and LDF during CCA occlusion

Figure 3a shows the CBF responses to CCA clipping/unclipping in a mouse forebrain measured concurrently by the LDF (top panel) and DCS (bottom panel). The CBF responses to CCA clipping/unclipping measured by the two techniques are highly synchronized. As expected, CBF decreased remarkably when LCCA was first clipped, then reduced further to minimum values after RCCA was clipped. Following the release of bi-CCA clippings CBF restored

towards the baselines. Substantial CBF changes were observed again during the second bi-CCA clipping/unclipping. Note that the LDF measurement is sensitive to motions, which can be seen from the motion artifacts in the top panel of Fig. 3a. This is anticipated because the gluing of tiny and flexible LDF probe (~0.25 mm in diameter [47]) to a small branch of MCA (< 0.15 mm in diameter [48]) is susceptible to the motion of probe or mouse head during surgical procedures. By contrast, the DCS flow measurement is more robust because DCS probes a large volume of tissue microvasculature and its outcome represents an average CBF from bulk tissues [26]. The LDF data with motion artifacts (CBF is above 100% larger than its adjacent values) are excluded from the data analysis and the correlations between the two measurements are investigated. Figure 3b shows the linear regressions of CBF measured by the LDF and DCS, where the LDF data with a high sampling rate (~32 Hz) are re-adjusted via an averaging method to align with the DCS data with a low sampling rate (0.4 Hz). The CBF changes (with all data sets) measured by the two techniques are highly correlated ($R^2 = 0.94$, $p < 0.0001$), although the regression slope (1.40) and interception (14.23) are different from the expected values. Theoretically, the regression slope and interception should be 1 and 0 respectively if both techniques measured the same quantity (i.e., CBF) over the same tissue volume. Nevertheless, the CBF reductions due to CCA clippings (i.e., the sub-data sets with $CBF < 100\%$) measured by the two techniques demonstrate a good consistence (slope = 1.06, interception = 0.84), as shown in the small inset plot in Fig. 3b. Interpretations about the consistence/inconsistence between the two measurements can be found in Section 4.

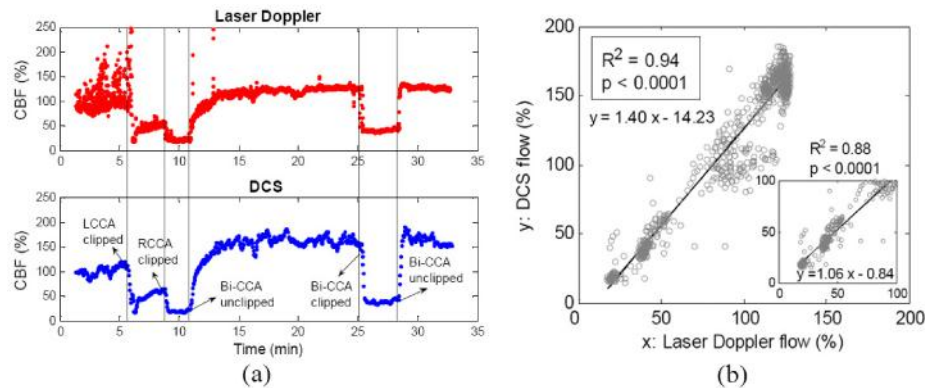


Fig. 3. (a) The CBF changes during unilateral clipping and bi-CCA clipping/unclipping (twice) measured by the laser Doppler (top panel) and DCS (bottom panel). (b) The linear regressions of CBF changes measured by the laser Doppler and DCS. The CBF changes measured by the two techniques are highly correlated ($R^2 = 0.94$, $p < 0.0001$). The inset small plot shows a linear regression of the CBFs with sub-data sets during arterial clippings ($CBF < 100\%$).

3.2 Protocol #2: regional and global CBF measurements during CCA occlusion

Figure 4a shows the regional (in each hemisphere) and global (across two hemispheres) CBF responses in a mouse during transient forebrain ischemia (I-R challenge). When RCCA was ligated, the regional CBF in right hemisphere decreased remarkably whereas the CBF in left hemisphere kept almost constant. The subsequent LCCA clipping caused further CBF decreases in both hemispheres because the cerebral blood inflows were almost fully blocked. Following the unclipping of LCCA, CBF increased substantially in both hemispheres. However, the CBF in right hemisphere was still lower than its pre-clipping baseline value due to the permanent ligation of RCCA. The global CBF was approximately the mean value of left and right CBFs throughout the CCA clipping/unclipping, suggesting the consistent relationship between the regional and global CBFs.

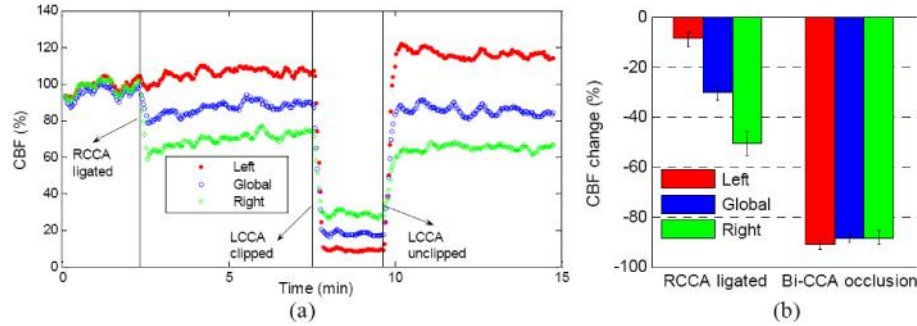


Fig. 4. (a) The regional (left and right hemispheres) and global (across two hemispheres) CBF responses to unilateral and bi-CCA occlusions in a mouse brain measured by DCS flow-oximeter. (b) The average regional and global CBF changes over 9 mice during unilateral (RCCA ligated) and bilateral CCA (LCCA clipped) occlusions.

Ten mice were measured in this protocol. Although inter-subject variation existed, the mice exhibited a consistent CBF response pattern as shown in Fig. 4a. Figure 4b shows the average CBF reductions during unilateral (RCCA) and bilateral CCA occlusions over all mice except Mouse #1. According to DCS measurements, the CBF reduction during bi-CCA occlusion in Mouse #1 (global CBF change = -65.6%) was much less than other mice ($-79.5\% \sim -94.2\%$). The ischemic procedure in this mouse was considered incomplete and the corresponding data were excluded for averaging. On average ($n = 9$), the CBF reductions in left ($-8.8 \pm 2.9\%$), global ($-30.3 \pm 3.3\%$) and right ($-50.7 \pm 4.7\%$) hemispheres following the RCCA ligations were significantly different ($p < 0.005$), whereas they were similar ($-91.3 \pm 1.4\%$, $-88.5 \pm 1.6\%$ and $-86.6 \pm 3.1\%$, respectively) during bi-CCA occlusions ($p > 0.3$).

3.3 Protocol #3: simultaneous measurements of CBF and cerebral blood oxygenation during repeated transient forebrain ischemia

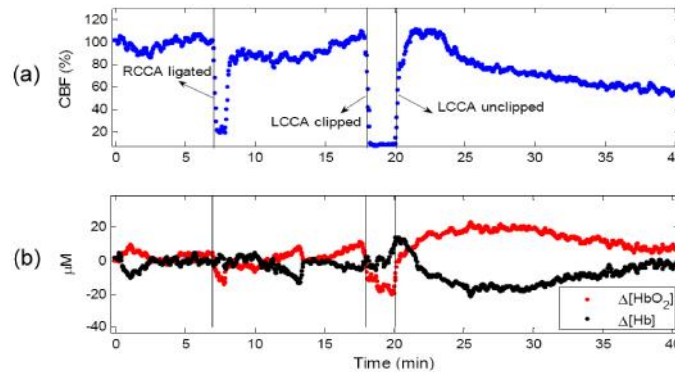


Fig. 5. The CBF (a), $\Delta[\text{HbO}_2]$ and $\Delta[\text{Hb}]$ (b) responses to unilateral and bi-CCA occlusions in a mouse brain measured by DCS flow-oximeter.

Figure 5 shows the global changes of CBF, $\Delta[\text{HbO}_2]$ and $\Delta[\text{Hb}]$ during CCA occlusion measured at Day 1 in a mouse. Note that DCS flow measurements were found not sensitive to the variation in wavelength [40, 49], thus the CBF data obtained from only one wavelength (785 nm) are presented. The permanent RCCA ligation resulted in a sharp decrease ($\sim -80\%$) followed by a rapid increase of CBF (see Fig. 5a). A gradual and continuous restoration of CBF towards its baseline was then observed. The sharp increase and gradual restoration in CBF were likely due to the CBF compensation from the contralateral (unclipped) hemisphere via circle of Willis [50]. Correspondingly, the $\Delta[\text{HbO}_2]$ decreased quickly at the beginning of RCCA ligation, then recovered towards its baseline (see Fig. 5b). During the 2-minute bi-CCA

occlusion, the CBF sharply decreased by ~90% (Fig. 5a), resulting in a decrease in $\Delta[\text{HbO}_2]$ and an increase in $\Delta[\text{Hb}]$ (Fig. 5b). Following the release of LCCA clipping, the CBF and cerebral oxygenation recovered towards their baselines respectively although the CBF level didn't restore completely to its baseline value.

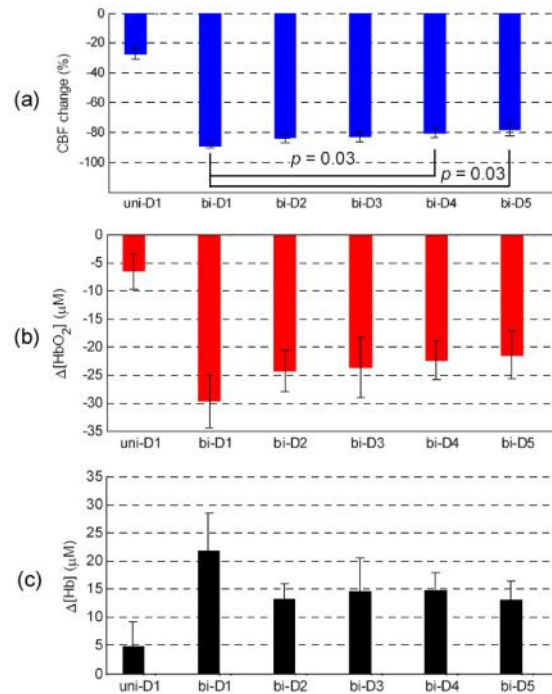


Fig. 6. The average changes over 8 mice in CBF (a), $\Delta[\text{HbO}_2]$ (b) and $\Delta[\text{Hb}]$ (c) during 5-day (D1 to D5) repeated transient I-R challenges.

Ten mice received a 2-minute I-R challenge repeatedly once per day up to 5 days using the unique procedure described in Section 2.2. Eight out of ten mice survived at the end of the experiments. Two mice exhibited severe stroke symptoms at Day 3 and Day 4 respectively. Thromboses were found in ligated CCAs and infarcts were found in ipsilateral brains, which were likely due to the mechanical vascular damage or the formation of thrombus during the repeated stops of blood flow during ischemia. Since the stroke symptoms can affect cerebral responses to I-R challenges, these two mice were excluded from this protocol. Although variations among subjects existed, similar CBF response patterns were observed (see Fig. 5). Figure 6 shows the average changes ($n = 8$) in CBF and cerebral oxygenation during the unilateral CCA ligations at Day 1 (Uni-D1) and during the repeated bi-CCA occlusions over five days (Bi-D1-5). At Day 1, the unilateral (RCCA) ligations caused relatively smaller reductions in both CBF ($-27.1 \pm 3.7\%$) and oxygenation ($-6.6 \pm 3.2 \mu\text{M}$ in $\Delta[\text{HbO}_2]$ and $+5.0 \pm 4.3 \mu\text{M}$ in $\Delta[\text{Hb}]$); whereas the bi-CCA occlusions resulted in larger changes in cerebral hemodynamics ($-89.2 \pm 1.7\%$ in CBF, $-29.8 \pm 4.7 \mu\text{M}$ in $\Delta[\text{HbO}_2]$, and $+21.9 \pm 6.7 \mu\text{M}$ in $\Delta[\text{Hb}]$). With the increase of I-R challenging cycles, the magnitudes of CBF reductions during 2-minute bi-CCA occlusions declined (see Fig. 6a). For example, CBF reductions at Day 4 (Bi-D4) and Day 5 (Bi-D5) were significant less ($p = 0.03$) than that at Day 1 (Bi-D1). The average oxygenation changes (up to $-24.3 \mu\text{M}$ in $\Delta[\text{HbO}_2]$ and $+14.9 \mu\text{M}$ in $\Delta[\text{Hb}]$) induced by the 2-minute bi-CCA occlusion at Day 2-5 (Bi-D2-5) were also remarkably smaller than those ($-29.8 \mu\text{M}$ in $\Delta[\text{HbO}_2]$ and $+21.9 \mu\text{M}$ in $\Delta[\text{Hb}]$) at Day 1 (Bi-D1), although these differences were not statistically significant ($p > 0.2$) due to the large inter-subject variations (see the large error bars in Fig. 6b and Fig. 6c).

4. Discussion

Real-time monitoring of CBF and cerebral oxygenation is appealing in mouse stroke studies, as it provides a direct and objective way to instantly judge the success of arterial clippings for inducing cerebral ischemia and to continuously assess cerebral hemodynamic responses. The alterations in CBF/cerebral oxygenation during cerebral arterial occlusions reflect the tolerance or injury of brain to hypoperfusion/hypoxia that is closely associated with pathophysiological outcomes of stroke. Quantification of cerebral hemodynamic changes during cerebral ischemia may provide useful information for evaluating the preconditioning/TIA in protection/promotion of stroke. The present study has successfully adapted an innovative DCS flow-oximeter for longitudinally assessing cerebral hemodynamics in mice with transient forebrain ischemia. The portable DCS flow-oximeter (see Fig. 1) is novel in that it can simultaneously quantify CBF and cerebral oxygenation in deep mouse brain, thus allowing for a comprehensive evaluation of cerebral ischemia and tissue hypoxia.

Several experimental protocols (see Section 2.3) were designed to compare DCS with LDF for CBF measurements and to test the capability and sensitivity of DCS flow-oximeter in detecting cerebral hypoperfusion and hypoxia in mice undergoing repeated transient forebrain ischemia. Several fiber-optic probes (see Fig. 2) were developed to meet the special needs of the designed experiments. The removal of mouse scalp ensured the good installation of optical probes on the exposed skull and avoided the partial volume effect from the overlying scalp tissues. The minimally-invasive surgery for removing mouse scalp did not show obvious influence on mouse daily activities. For the validation study, DCS shared the LDF source (see Fig. 2a) to avoid the light interference between the two measurements. This integrated probe design made the fiber arrangement easy and synchronized the two measurements precisely. By placing multiple pairs of S-D fibers at the two sides of mouse head (see Fig. 2b), the regional and global CBFs can be measured simultaneously. For the longitudinal monitoring of repeated ischemic mice over days, the optical fibers were confined in a foam pad that was permanently glued on the mouse skull (see Fig. 2c). The optical fibers can be easily inserted into or removed off the foam pad based on the experimental needs. This unique design for flexibility permits the longitudinal measurements at the same location of mouse brain without significantly interrupting mouse daily activities.

Using Protocol #1, the CBFs measured by DCS and LDF are compared. LDF exhibits a high sensitivity to motions of the probe and animal head (see Fig. 3a) and has difficulty in aligning its tiny probe on a small vessel. By contrast, DCS measurement is more robust and easier to implement. The CBF changes during multiple I-R challenges measured by the two techniques are highly correlated (see Fig. 3b). Interestingly, the CBF reductions during CCA clippings (CBF < 100%) measured by the two techniques are found highly consistent (regression slope = 1.06, see the small inset plot in Fig. 3b) whereas CBF increases after the release of CCA clippings (CBF > 100%) are slightly different (regression slope > 1, see Fig. 3b). The CCA occlusions completely cut off the blood supply to the entire brain, thus reduce the CBF to the same amount in both superficial cortex (detected by LDF) and deep brain (detected by DCS). However, the flow reperfusion after the release of CCA clippings (CBF increase) depends on the vasodilatation capacities of the measured vessels. The deep brain microvasculature may have larger vasodilatation capacity than the superficial single vessel, thus producing higher DCS reperfusion signals originated from deep brain tissues. Other differences between LDF and DCS may also contribute to the CBF measurement discrepancy, including those in analytical models (single scattering versus multiple scattering) [26, 47], measured vessels (single superficial vessel versus deep microvasculature bed), and probed tissue volumes (tiny spot versus bulk tissues). Similar discrepancy in CBF measurements between DCS and LDF was also observed previously in rat brains under hypocapnia challenges [26]. Notice however that this pilot study compared the DCS and laser Doppler measurements

in only one mouse. Further investigations in a large population are needed to draw solid conclusions.

Protocol #2 tests the capability of dual-wavelength DCS for simultaneously monitoring the regional (left and right hemispheres) and global (across hemispheres) CBF changes in mice during unilateral and bilateral CCA occlusions. The unilateral CCA ligation induces a large CBF decrease ($-50.7 \pm 4.7\%$) in ipsilateral (clipped) hemisphere. Meanwhile a relatively small CBF reduction ($-8.8 \pm 2.9\%$) in contralateral (unclipped) hemisphere can be simultaneously detected by the DCS flow-oximeter (see Fig. 4). The small CBF reduction in the unclipped hemisphere is likely due to collateral compensation effects. As expected, bi-CCA occlusion results in further decreases in both regional and global CBFs. The global CBF across the hemispheres is approximately equal to the average value of the regional CBFs in two hemispheres (see Fig. 4b), demonstrating the accuracy of DCS in detecting both regional and global CBF changes. Since neurological injury and cell loss often appear locally in the ischemic brain and are closely associated with the local ischemic status, monitoring of the regional CBF may assist in evaluating *in situ* neurological infarct and tissue damage.

Protocol #3 is designed to exam the ability of DCS flow-oximeter for simultaneously monitoring CBF and cerebral oxygenation changes in mice undergoing repeated transient forebrain ischemia. As expected, the CCA clipping/unclipping induces instant CBF decrease/increase, leading to cerebral deoxygenation/reoxygenation (see Fig. 5 and Fig. 6). Similar to the results obtained from Protocol #2 (see Fig. 4b), the unilateral CCA ligation at Day 1 induces less CBF changes than bi-CCA occlusions, leading to smaller variations in cerebral oxygenation. DCS flow-oximeter demonstrates high sensitivities in detecting these anticipated hemodynamic changes. Currently, there are only a few published studies measuring both blood flow and oxygenation in rat brains during one-time MCA occlusions [17, 28, 51]. For comparisons, we calculate the relative oxygenation changes driven by the CBF reduction during bi-CCA occlusions at Day 1 (see Fig. 6): $\Delta[\text{HbO}_2]/\Delta\text{CBF} = 0.34 \pm 0.06 \mu\text{M}/\%$ and $\Delta[\text{Hb}]/\Delta\text{CBF} = -0.25 \pm 0.08 \mu\text{M}/\%$. These ratios fall respectively in the ranges of hemodynamic responses extracted from the reported data [28, 51]: $\Delta[\text{HbO}_2]/\Delta\text{CBF} = 0.19$ to $0.52 \mu\text{M}/\%$ and $\Delta[\text{Hb}]/\Delta\text{CBF} = -0.19$ to $-0.31 \mu\text{M}/\%$. Since cell death results primarily from the lack of tissue oxygen, nutrients supply and waste exchanges, simultaneous monitoring of cerebral oxygenation and CBF during cerebral ischemia provides the deep insight about the pathophysiology of cerebral tissue damage. Moreover, simultaneous hemodynamic measurements allows for an estimation of cerebral oxygen metabolism [28]. This metabolic index is potentially a more direct indicator of tissue metabolic activities and provides further insight about tissue physiology/pathophysiology.

Using the special probe design and unique mouse model created in the present study, cerebral hemodynamic changes in mice during repeated 2-minute transient I-R challenges (bi-CCA occlusions) have been successfully monitored over 5 days. Note that two out of ten mice involved in this protocol were excluded from the data analysis due to their severe stroke symptoms in the middle of experiments. The 20% unsuccessful rate is not surprising considering the complexity of multiple I-R circles over days. One important finding from this protocol is that cerebral hemodynamic alternations during transient forebrain ischemia decrease with the progress of repeated short-term I-R challenges (see Fig. 6). More specifically, the magnitudes of CBF reductions at the last two days (Day 4-5) are significantly smaller than that at the first day (Day 1). Correspondingly, the oxygenation changes at Day 2-5 are also remarkably smaller than those at Day 1. One likely reason for these longitudinal changes is that the repeated short-term intermittent interruptions of CBF (preconditioning) enhance the cerebral blood supply from other branches, thus compensating the flow loss caused by the CCA occlusions. Furthermore, the repeated short-term I-R challenges may also enhance the cerebral ischemic tolerance. These observations imply that mouse adaptation to cerebral ischemia could be influenced by the repeated preconditioning.

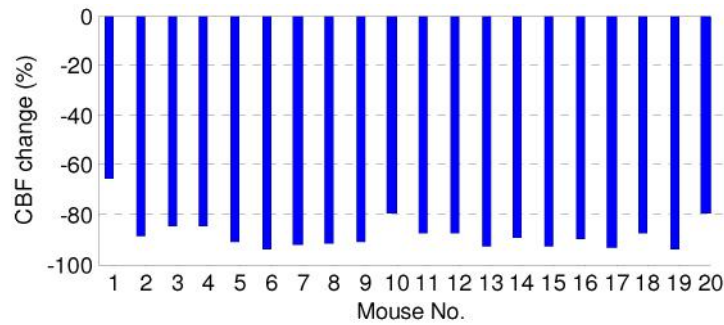


Fig. 7. The CBF changes during bi-CCA occlusions in 20 mice involved in Protocol #2 and Protocol #3 at Day 1. Mouse #1-10 and Mouse# 11-20 were measured in Protocol #2 and Protocol #3, respectively. Three mice were eventually excluded from statistical analysis due to the incomplete ischemic response (Mouse #1) or severe stroke symptoms (Mouse #17 and #18).

For precise evaluation and comparison of ischemic effects in different mice, it is critical to induce a complete forebrain ischemia in all subjects through the bi-CCA occlusions. Although well-trained surgeons may be able to judge the success of a bi-CCA occlusion based on their experience, the heterogeneity of animal responses to arterial occlusion cannot be ruled out. Figure 7 shows the global CBF reductions during 2-minute bi-CCA occlusions for all 20 mice measured in Protocol #2 and Protocol #3 (at Day 1). Inter-subject variation in CBF reductions exists although all mice receive identical surgical procedures. Particularly, Mouse #1 demonstrates a much less CBF reduction (-65.6%) during the bi-CCA occlusion compared to other mice. The less CBF reduction in this mouse might result from the pre-existed enriched collateral blood flow or improper installation of arterial occluder. Mouse #1 is thus excluded from the data analysis due to its incomplete response to the arterial occlusion. By contrast, the global CBF reductions in all other 19 mice (except Mouse #1) are consistently larger than 75% (see Fig. 7). Therefore, the 75% CBF reduction may be considered as a threshold to determine a successful bi-CCA occlusion. Further investigations correlating the CBF reductions with behavioral tests and histological outcomes in ischemic mice are needed to verify this ischemic threshold. This threshold is within the range of CBF reductions following bi-CCA occlusions observed in mice [8, 9] and rats [52] that were measured by laser Doppler. However, considering the advantages of DCS over laser Doppler as discussed early, DCS is expected to be a robust and easy-to-use tool for objectively assessing the success of cerebral ischemia in mice. In contrast to the consistent large CBF reductions following bi-CCA occlusions, CBF responses to unilateral CCA occlusions vary largely among mice (see Figs. 3-6). Following an initial rapid CBF reduction caused by the unilateral CCA ligation, the CBF in the ipsilateral (occluded) hemisphere either recovers towards its baseline (see Fig. 5a) or remains at a lower level than its baseline (see Fig. 4a). The distinct flow responses in different mice are likely due to the compensatory CBFs from the contralateral (non-occluded) hemispheres, which rely on integrity of the circle of Willis [50]. As a result, the CBFs in the contralateral hemispheres also exhibit variations although they are smaller than the ipsilateral hemispheres (see Fig. 4). The interruptions of CBF in both hemispheres during unilateral CCA occlusions result in corresponding changes in cerebral oxygenation. The large inter-subject heterogeneities in regional hemodynamic responses further emphasize the necessity to monitor CBF and cerebral oxygenation in both hemispheres for each individual mouse.

The dual-wavelength DCS flow-oximeter used in the present study has two laser sources (785 and 854 nm), which allow for simultaneous measurements of either regional CBFs in the two hemispheres (see Fig. 2b), or global CBF and oxygenation across the two hemispheres (see Fig. 2c). In order to monitor both CBF and oxygenation in the two hemispheres, a second pair of lasers (785 and 854 nm) must be added into the current dual-wavelength DCS flow-oximeter system, which will be the subject of future work.

To conclude, the novel DCS flow-oximeter has been successfully adapted for simultaneous monitoring of CBF and cerebral oxygenation in mouse brains. DCS for mouse CBF measurement correlates well with LDF, and is less susceptible to motion artifacts. With the unique designs in experimental protocols and corresponding fiber-optic probes, the present study has demonstrated high sensitivities of DCS flow-oximeter in detecting the regional/global changes of CBF and cerebral oxygenation in mice undergoing multi-day repeated transient forebrain ischemia (2-minute bi-CCA occlusion). Monitoring of regional cerebral hemodynamics in each of the two hemispheres provides information for evaluating the collateral compensation effects during unilateral CCA occlusion and for potentially estimating the *in situ* neurological deficits and tissue damages. Simultaneous measurements of CBF and cerebral oxygenation allow for comprehensively assessing cerebral ischemia and tissue hypoxia during cerebral arterial occlusion. DCS flow-oximeter measurements permit real-time quantification of cerebral hemodynamic responses to transient forebrain ischemia, which can be used to guide proper arterial occlusion and evaluate the preconditioning effects on brain adaptation to cerebral ischemia. More than 75% CBF reductions were found during bi-CCA occlusions in mice, which may be considered as a threshold to determine a successful bi-CCA occlusion. The longitudinal declines in CBF reductions during the 2-minute short-term I-R challenges indicate that mouse adaptation to cerebral ischemia could be influenced by the repeated preconditioning. Future studies will evaluate TIA-induced injury to brain through applying repeated medium-term I-R challenges (e.g., 10-min bi-CCA occlusions) to mice. The cerebral hemodynamic changes during repeated transient/medium I-R challenges will be compared with pathophysiological consequences (e.g., neurologic deficits, stroke volumes) of stroke manipulated by permanent MCA occlusions. The anticipated correlations between the cerebral hemodynamic responses and physiological consequences would provide deep insights about the preconditioning/TIA mechanism in protection/promotion of stroke.

Acknowledgments

This work was partially supported by the grants from American Heart Association Great Rivers Affiliate including BGIA #2350015 (GY) and Postdoctoral Fellowship Awards #11POST7360020 (YS) and #09POST2370028 (LC), and the grants from NIH including DA027569 (MT) and CA133257 (MT).